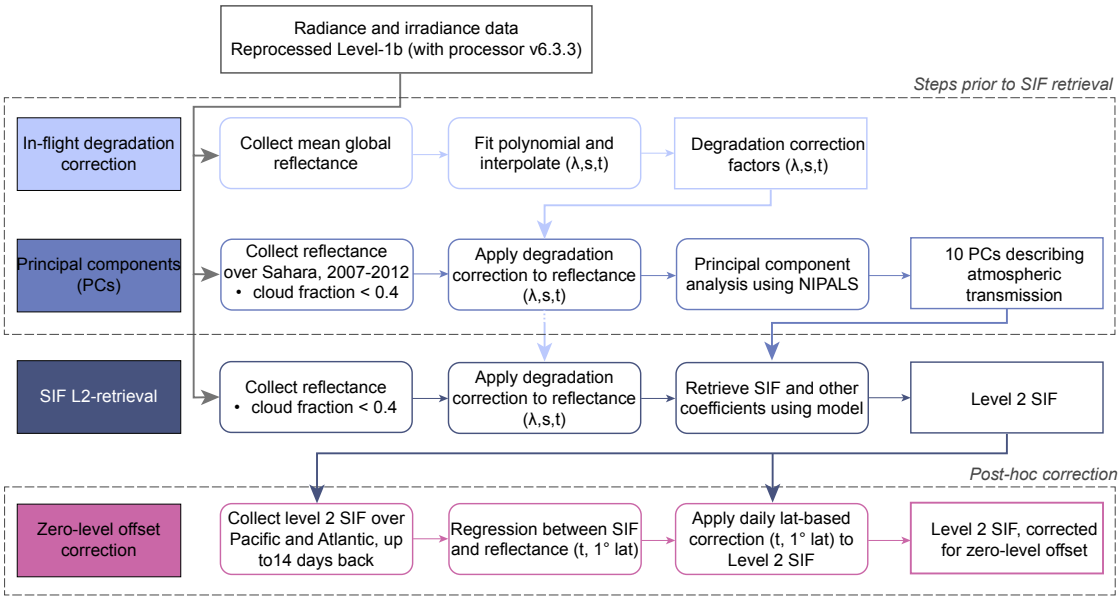

Figure S1. Flowchart showing the basic steps to retrieve Level-2 SIF from GOME-2A using the SIFTER v3 algorithm.

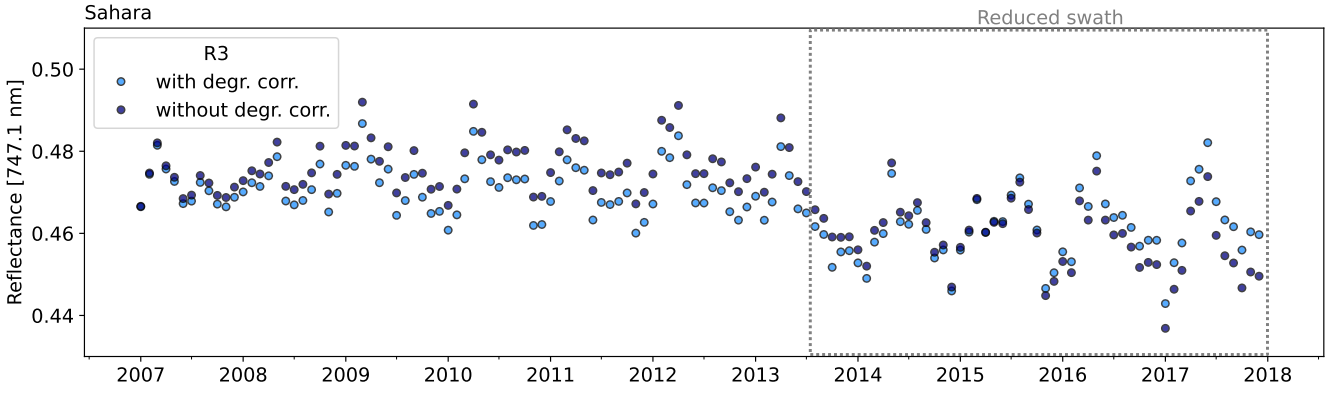

Figure S2. Time series of monthly averaged level-1b Release 3 (R3) reflectance data at 747.1 nm over the Sahara including (denoted in blue) and excluding (denoted in navy) the in-flight degradation correction. The reduced swath period is indicated by the dashed box.

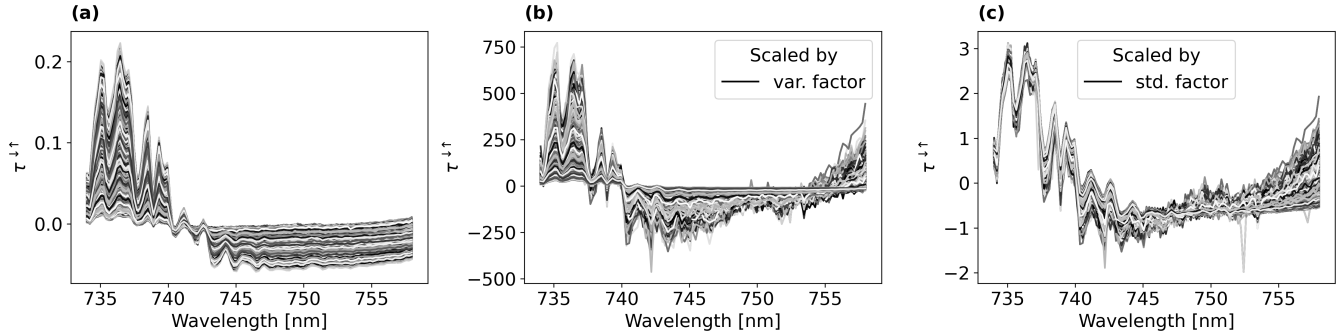

Figure S3. (a) Centralized two-way slant absorption optical thickness $\tau^{\uparrow\downarrow}$ spectra over the Sahara reference area between 2007 and 2012. Panels (b) and (c) show the centralized and scaled spectra, scaled by the variance and standard deviation factor, respectively.

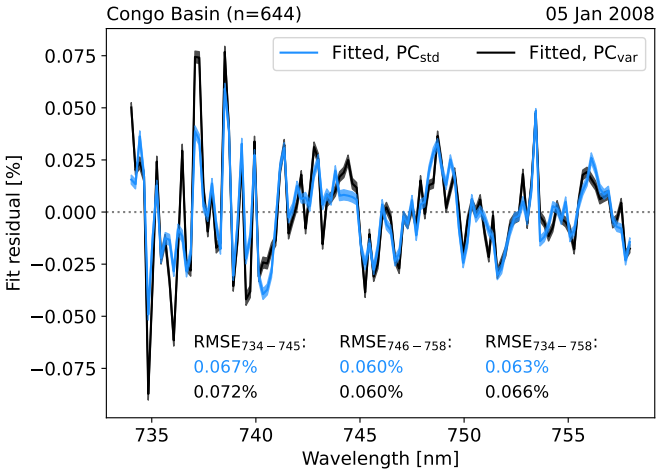

Figure S4. Average fit residuals of 644 pixels over the Congo Basin at 5 January 2008 obtained with PCs that used standard deviation scaling (denoted in blue) and PCs that used variance scaling (denoted in black). All other settings follow that of SIFTER v3.

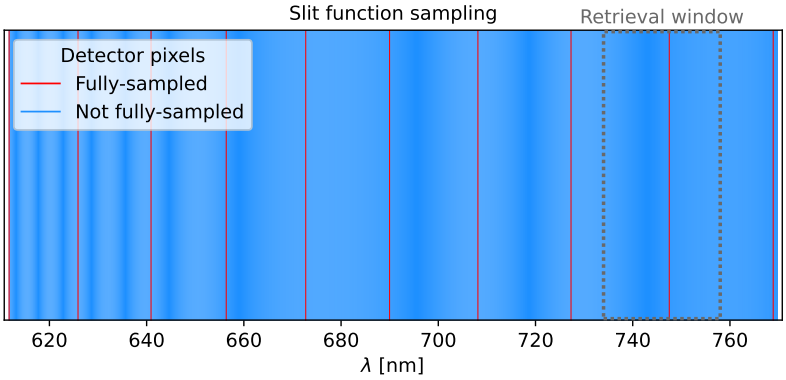

Figure S5. Location of all fully and not-fully sampled pixels that contain slit function information. The SIF retrieval window is indicated by the grey dashed line.

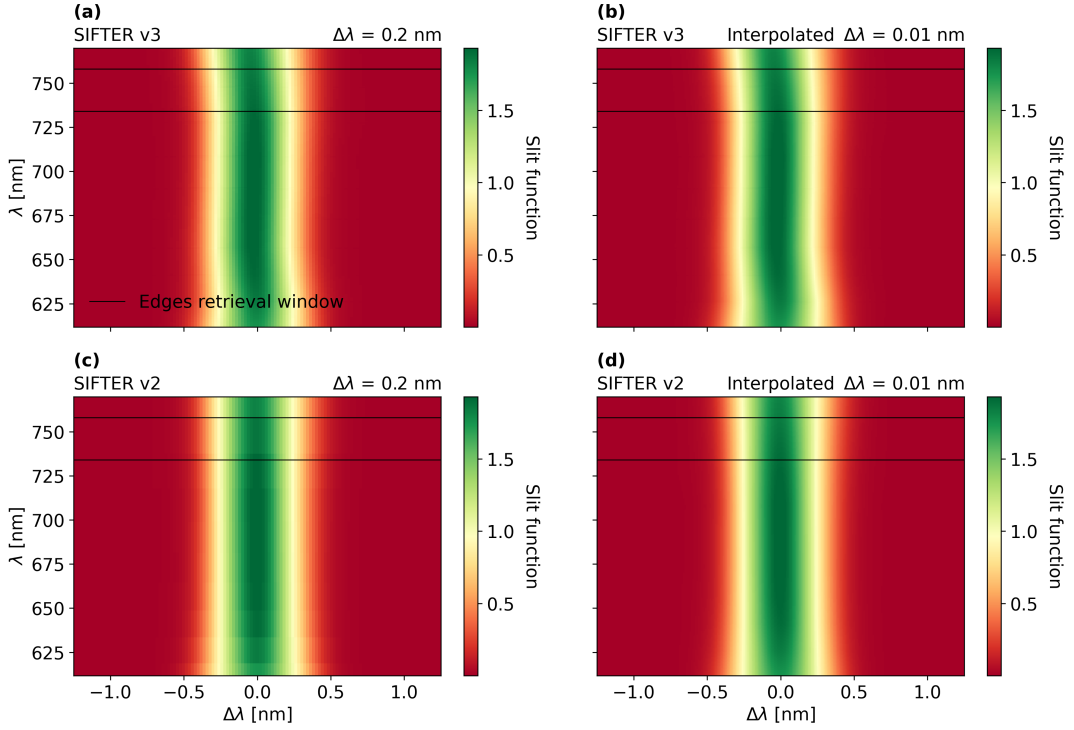

Figure S6. Slit functions of all (a) fully and not-fully sampled detector pixels (n=765), as done in SIFTER v3, and (c) only fully sampled detector pixels (n=10), as done in SIFTER v2, with the spectral resolution of 0.2 nm. The two right panels show the results of the interpolation across the slit functions to the spectral resolution of Chance and Kurucz at 0.01 nm, using (b) all pixels as input and (d) only the fully-sampled pixels as input.

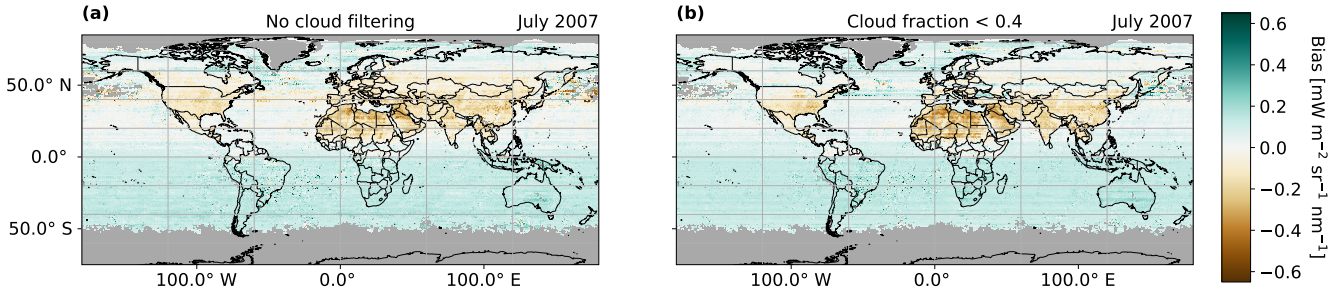

Figure S7. Gridded zero-level adjustment biases ($0.5^\circ \times 0.5^\circ$) over July 2007 of SIFTER v3 (a) without cloud filtering and (b) with pixels that met the criteria of cloud fractions <0.4 (as done in SIFTER v2).

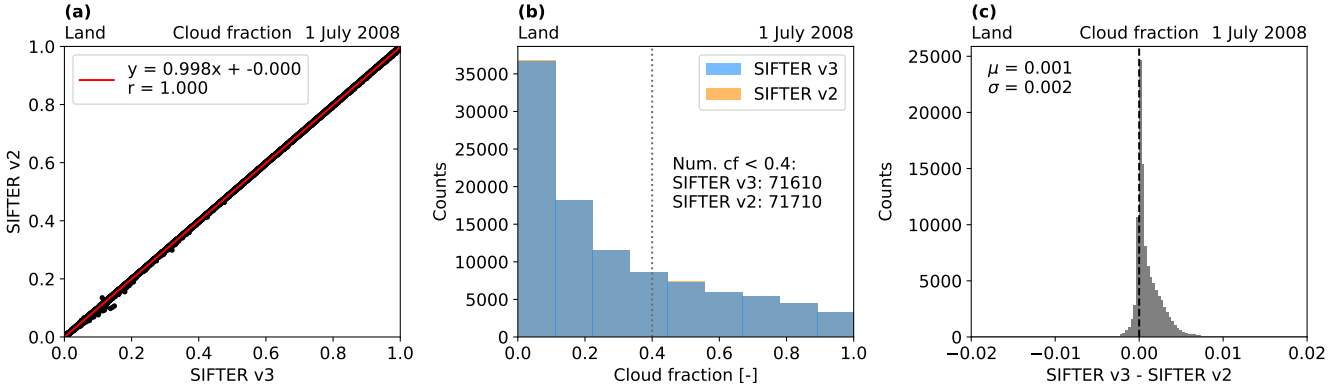

Figure S8. Difference in cloud fractions of SIFTER v3 and SIFTER 2, due to different versions of FRESCO+. Pixel-by-pixel comparisons of the (a) comparison of the cloud fractions in both products, (b) the histograms of both products and indicating the number of pixels that meet the criteria of <0.4, and (c) the difference between the cloud fraction in SIFTER v3 and SIFTER v2. All shown data represents land pixels at 1 July 2008.

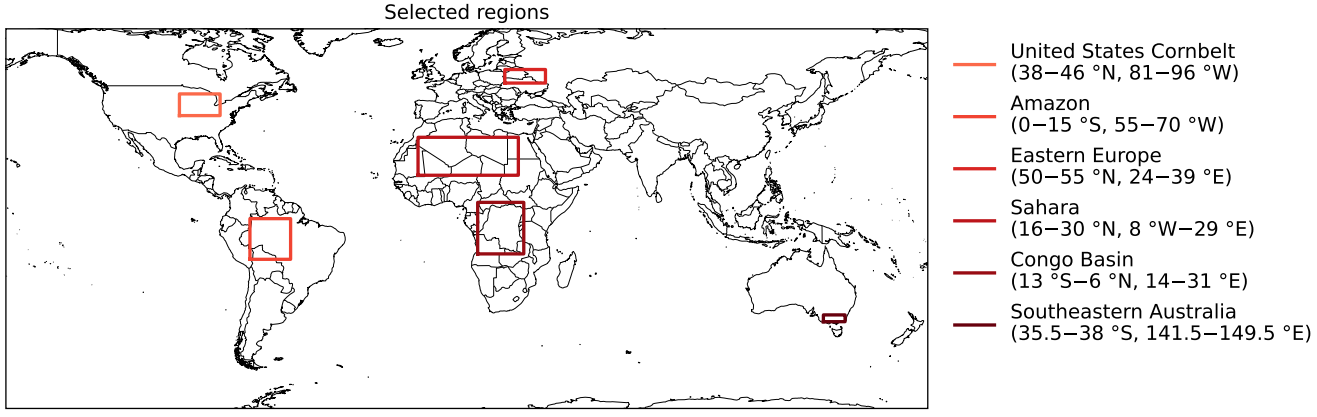

Figure S9. Locations of the selected regions in this study.

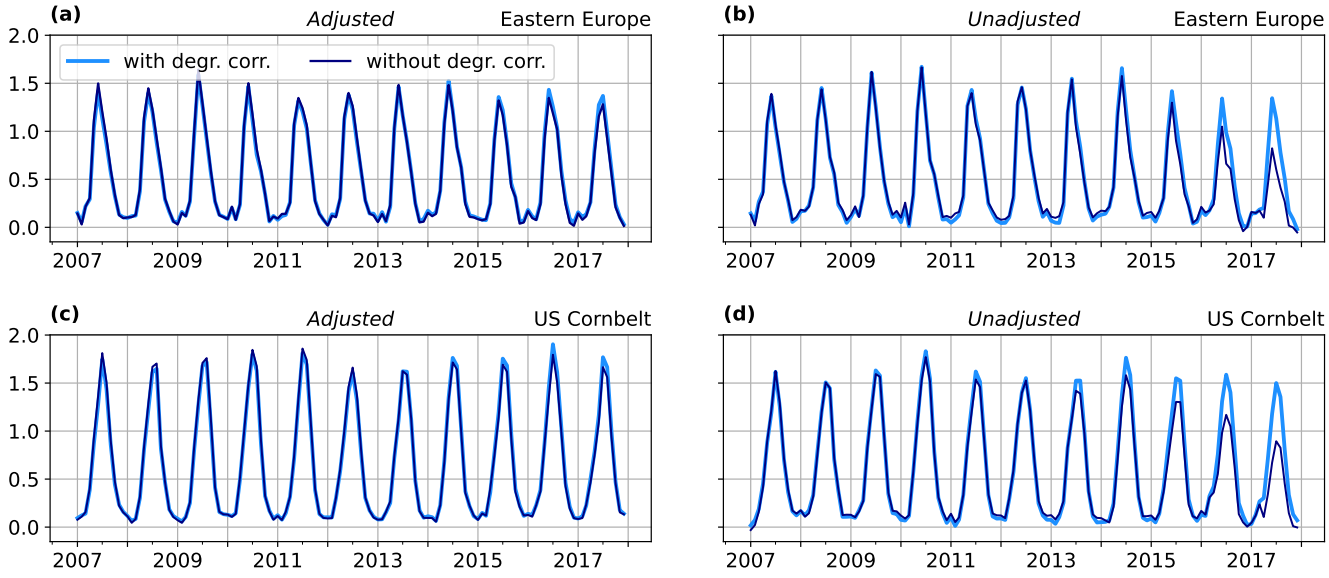

Figure S10. Time series of monthly averaged SIFTER v3 values over eastern Europe (a,b) and the US Cornbelt (c,d), with (denoted in light blue) and without (denoted in dark blue) applied degradation correction. The left panels (a,c) show the values for the final product, including the zero-level adjustment, the right panels (b,d) show the values for the retrieved SIF without the zero-level adjustment.

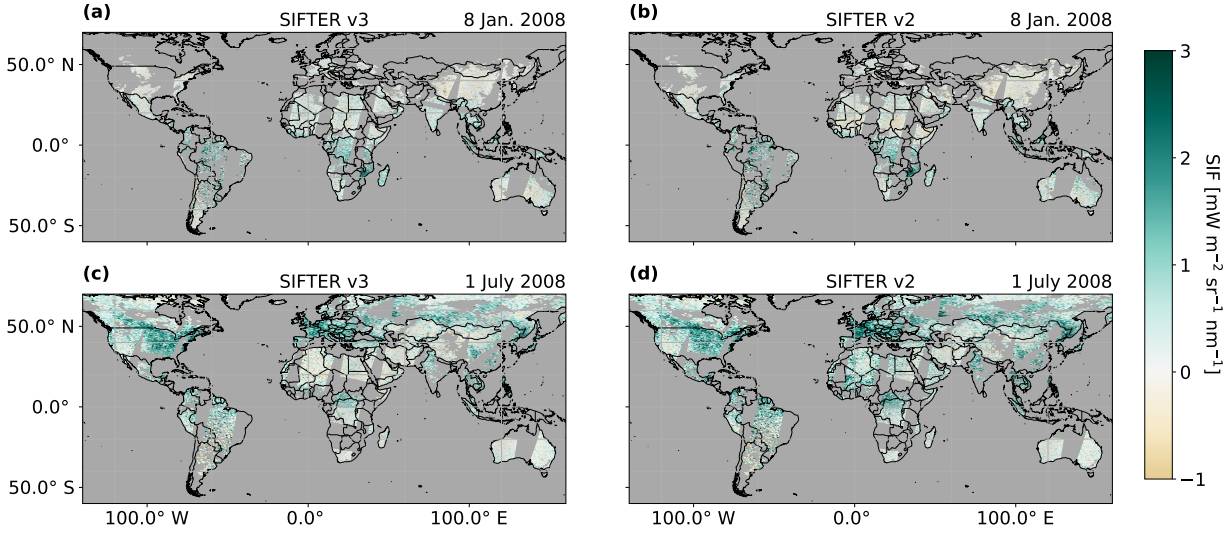

Figure S11. Gridded monthly mean GOME-2A SIF values ($0.5^\circ \times 0.5^\circ$) from SIFTER v3 (a,c) and SIFTER v2 (b,d) in January and July 2008. SIFTER data was selected for autocorrelation values <0.2 and cloud fraction <0.4.

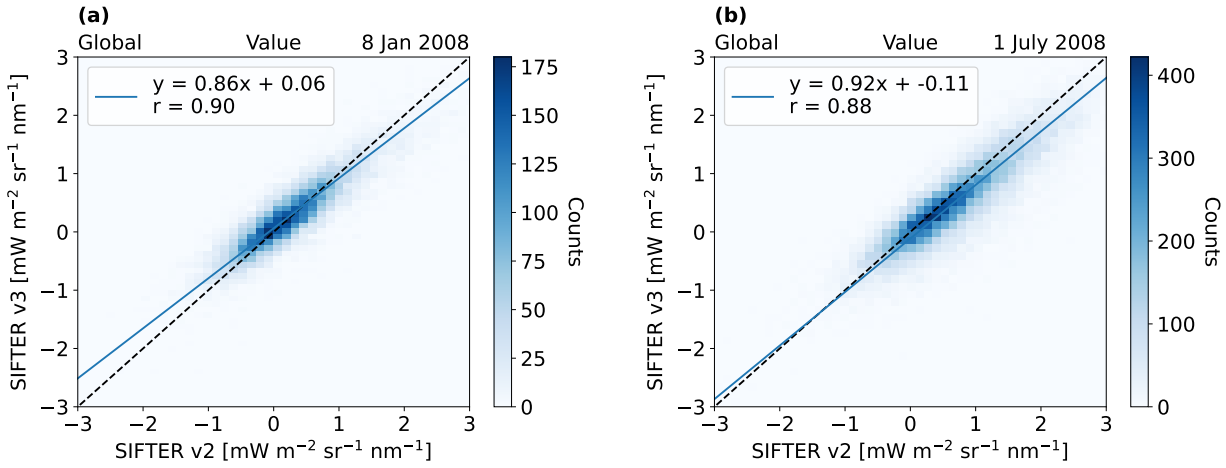

Figure S12. Pixel-by-pixel comparison of the SIF values of SIFTER v3 and SIFTER v2 over all land-pixels on (a) 8 Jan 2008 and on (b) 1 July 2008. The pixels cover the global land area and are filtered for autocorrelation values <0.2 and cloud fractions <0.4.

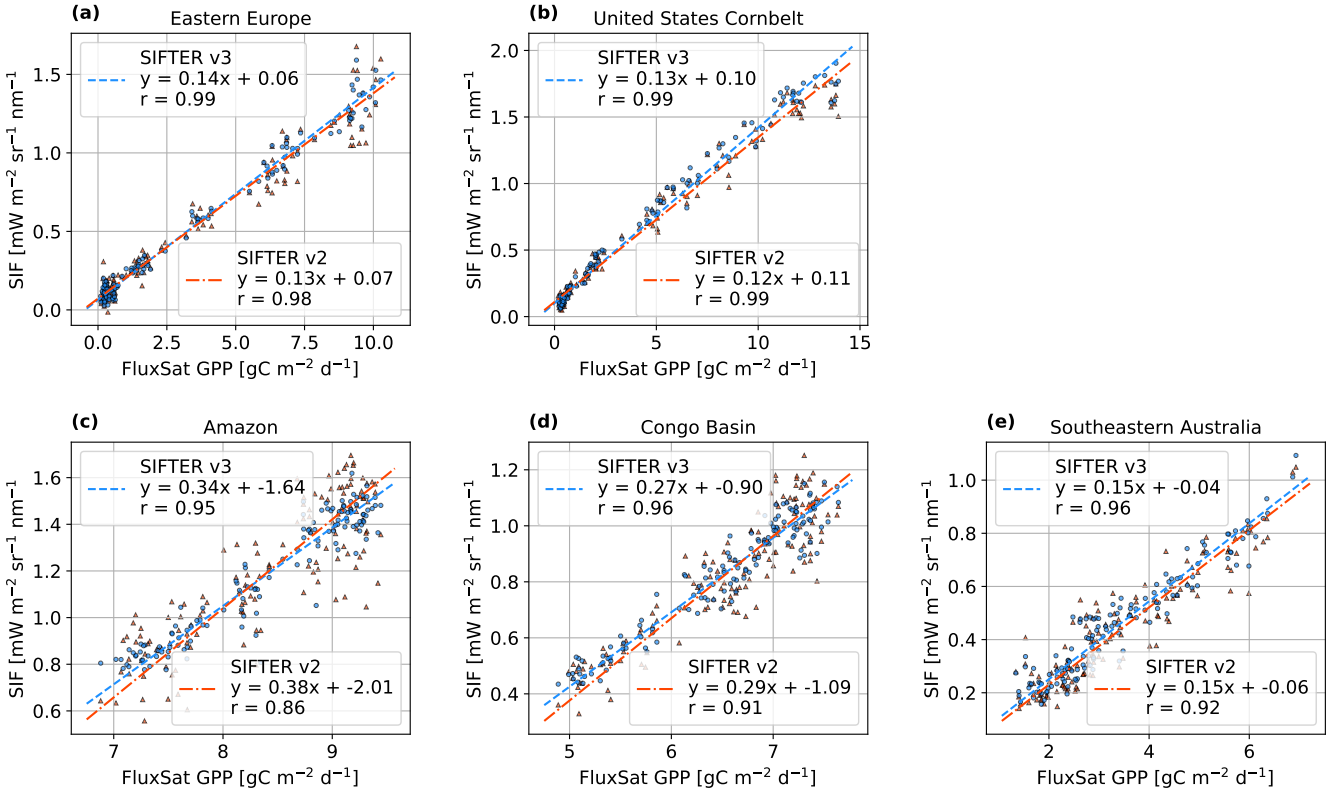

Figure S13. Comparison of monthly averaged FluxSat GPP with SIF data from SIFTER v3 (blue bullets) and SIFTER v2 (orange triangles) across (a) eastern Europe, (b) United States Cornbelt, (c) the Amazon, (d) the Congo Basin, and (e) southeastern Australia.

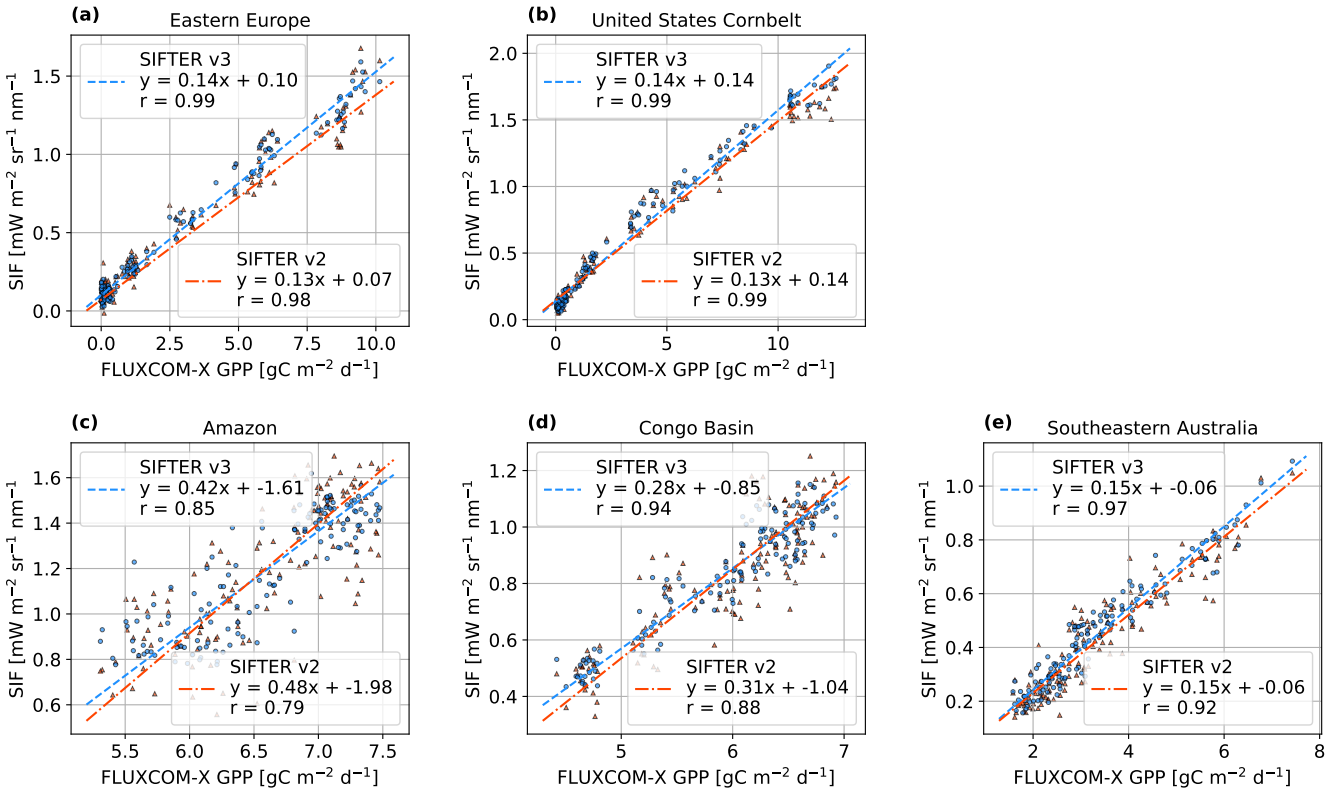

Figure S14. Comparison of monthly averaged FLUXCOM-X GPP with SIF data from SIFTER v3 (blue bullets) and SIFTER v2 (orange triangles) across (a) eastern Europe, (b) United States Cornbelt, (c) the Amazon, (d) the Congo Basin, and (e) southeastern Australia.